Photonic band structures for bi-dimensional metallic mesa gratings

Juliette Plouin, Elodie Richalot, Odile Picon
ESYCOM, Universite de Marne la Vallee, France
plouin@univ-mlv.fr

Mathieu Carras, Alfredo de Rossi
Thales Research and Technology, Palaiseau, France

Abstract: Photonic band properties are presented for a two-dimensional rectangular-groove grating of metal into air. The properties of the surface modes are shown and discussed with a perfect electric conductor, and compared to those of surface plasmons with real metal. The same structure is also studied with real metal in the near infrared. The results are obtained with a 3-D finite element numerical code.

OCIS codes: (230.1950) Diffraction gratings; (240.6680) Surface plasmons; (240.6690) Surface waves

References and links

1. E. Ozbay "Plasmonics: Merging Photonics and Electronics at Nanoscale Dimensions," Science **311**, pages 189-193 (2006).
2. S. C. Kitson, W. L. Barnes and J. R. Sambles, "Full photonic band gap for surface modes in the visible," Phys. Rev. Lett. **77**, 2670-2673 (1996).
3. J. Zhang, Y.-H. Ye, X. Wang, P. Rochon, and M. Xiao, "Coupling between semiconductor quantum dots and two-dimensional surface plasmons," Phys. Rev. B **72**, 201306 (2005).
4. M. Carras and A. De Rossi, "Field concentration by exciting surface defect modes," Opt. Lett. **31**, pages 47-49 (2006).
5. W.L. Barnes, A. Dereux and T.W. Ebbesen, "Surface plasmon subwavelength optics," Nature **424**, 824-830 (2003).
6. J. B. Pendry, L. Martin-Moreno, F.J. Garcia-Vidal, "Mimicking Surface Plasmons with Structured Surfaces," Science **305**, 847-848 (2004)
7. F.J. Garcia-Vidal, L. Martin-Moreno and J. B. Pendry, "Surfaces with holes in them : new plasmonic metamaterials," J. Opt. A:Pure Appl. Opt. **7**, S97-S101 (2004)
8. F.J. Garcia de Abajo and J.J. Saenz, "Electromagnetic surface modes in structured perfect-conductor surfaces," Phys. Rev. Lett. **95**, 233901-1-4 (2005).
9. Min Qiu, "Photonic band structures for surface waves on structured metal surfaces," Opt. Express **13**, 7583-7588 (2005).
10. A.P. Hibbins, B.R. Evans, J.R. Sambles, "Experimental Verification of Designer Surface Plasmons," Science **308**, 670-672 (2005).
11. W. Barnes, R. Sambles, "Only Skin Deep," Science **305**, 785-786 (2004).
12. W. L. Barnes, T. W. Preist, S. C. Kitson, J. R. Sambles, N.P.K. Cotter and D.J. Nash "Photonic gaps in the dispersion of surface plasmons on gratings," Phys. Rev. B **51**, 11 164-11 168 (1995).
13. W. L. Barnes, T. W. Preist, S. C. Kitson and J. R. Sambles, "Physical origin of photonic energy gaps in the propagation of surface plasmons on gratings," Phys. Rev. B **54**, 6227-6244 (1996).
14. A. Giannattasio and W. L. Barnes, "Direct observation of surface plasmon-polariton dispersion," Opt. Express **13**, 428-434 (2005).
15. M. Kretschmann "Phase diagrams of surface plasmon polaritonic crystals" Phys. Rev. B **68**, 125419 (2003).

#72206 - $15.00 USD Received 20 June 2006; revised 25 August 2006; accepted 26 August 2006

1. Introduction

Nanoscale patterning of metal surfaces is a very powerful technique, opening new perspectives in the field of photonics, such as ultra-compact photonic integrated circuits, new kinds of optical sources and sub-diffraction limited imaging [1]. In particular, a complete photonic band gap in the dispersion of surface plasmons (SPs) [2] is obtained through periodic patterning of metallic surfaces. These structures are the surface equivalent of photonic crystals. Instead of being confined inside a dielectric, the optical mode is in vacuum, although tightly bounded to the surface. These properties imply that the local density of photonic states is modified and so the emission from nanoscale optical sources (the Purcell effect). This effect was exploited to improve the emission properties of nanocrystals [3]. By combining double periodicity with a "defect" a surface concentration effect was predicted, which can be exploited in detection or emission enhancement from a point source[4].

A very intuitive picture for explaining the behavior of these periodically patterned surfaces could be used: a bound mode, the surface plasmon (SP), exists due to the plasmon resonance into the metal for a flat surface ; therefore, the periodic modification of the properties of the surface (e.g. by etching the metal layer, or modifying its profile) induces the Bragg scattering pretty much as holes do in dielectric photonic crystals. This perturbative approach is not adequate for understanding the more general properties of patterned surfaces. First of all, periodic patterning not only generates Bragg scattering, but also modifies the degree of confinement of the mode at the surface. Indeed, the mode of the low frequency band is more strongly confined (stronger extinction) than the SPs mode on a flat surface, while the high frequency band mode is less [12, 13]. This effect becomes stronger as the depth of the patterning increases ; moreover the SP effect is reduced when moving from the visible spectral range to the infrared. Thus, it is expected that the high-frequency band disappears below a cut-off frequency, which depends on the materials (metal and dielectric) and on the depth of the patterning. In any case, surface wave exists in any spectral range, even in the limit of perfect electric conductors (PEC), at least in 1D periodic structures defined on the x-y plane which are translation-invariant along z.

The case of 2D periodic surfaces in the 3D space is more complex. Very recently, Pendry made the connection between surface plasmons and surface waves on PEC surfaces with holes[6]. Indeed, the cut-off frequency in metallic holes acts as a plasmon resonance and evanescent penetration of the field in the holes mimics the skin effect. The experimental demonstration of such effect followed [10].

The recent literature on patterned PEC surfaces focuses on a specific geometry, that is plane PEC surfaces with sub-wavelength holes [7, 8, 9]. In this Paper we consider a complementary case, that is a plane PEC surface with bumps or other kind of protuberances forming a regular array. This is the case investigated experimentally [2] and theoretically [15] in the visible spectral range. We focus on the long wavelength limit and we will show that this structure supports surface waves and, depending on the depth of the patterning, more than one band under the air light line. We discuss the nature and the properties of such modes in the case of a rectangular lattice and compare the case of PEC structures with real metal in the near infrared. We also show how the properties of this band structure depend on geometric parameters, which can be controlled by surface designers.

2. Discussion

In our structure, the metal/dielectric interface consists in a two-dimensional rectangular-groove grating of metal into air, as shown in Fig. 1. The structure is symmetric, with the same period, Λ, in both orthogonal directions x and y. The bumps have a square cross-section $\alpha \times \alpha$, with height *h*.

We compute the photonic band structure by solving a suitable eigenvalue problem according

#72206 - $15.00 USD Received 20 June 2006; revised 25 August 2006; accepted 26 August 2006

Fig. 1. Structure of the metal coated two-dimensional array of squared bumps

to the Floquet-Bloch theorem. Thus, only one unit cell, with size $\Lambda \times \Lambda$, is simulated, limited by two lateral planes orthogonal to x direction and two others orthogonal to y direction. Boundary conditions imposed on two parallel lateral surfaces respect the field's property to be the same except for the phase, with a phase difference function of the wave vector. The eigenvalue problem is solved by HFSS (Ansoft), a 3-D finite-element commercial code. The height of the computational domain in the air is chosen to be large enough (equal to Λ) to ensure the existence of the surface modes, and to avoid artefact modes. We define Perfectly Matched Layers (PML) conditions in the z direction outside of the air domain. When non-perfect conductor is used, the metal is included in the computational domain and is meshed, and Perfect E boundary conditions are defined outside of the metal, to limit its thickness to $\frac{\Lambda}{15}$. The precision for eigenmode solutions in HFSS is given by the difference in the resonant frequencies from one adaptative solution to the next in the convergence process. The mesh size we used allowed a precision of 0.1% for PEC and 1% with real metal. To ensure that HFSS captures the physics associated with surface plasmons, we have computed the frequency of the SP constant on a metallic plane surface for metal with $\varepsilon_m = -50$. The theory predicts a propagation constant for a surface plasmon $k_{sp} = \frac{\omega}{c}\sqrt{\varepsilon_m/(\varepsilon_m+1)}$, corresponding to $f.\pi/(k_{sp}.c)$ = 0.495. The value calculated with HFSS is 0.497, which is reasonably close.

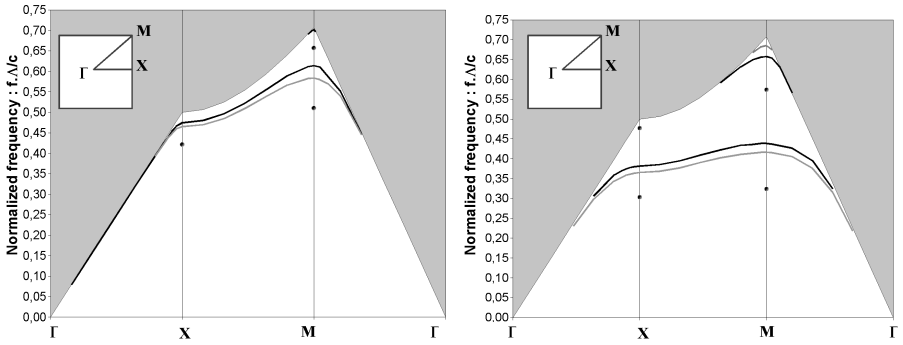

Fig. 2. Photonic bands of surface modes of structure in figure 1 with depth $h = 0.2 \times \Lambda$ (left) and $h = 0.4 \times \Lambda$ (right). The thick dark lines correspond to $\alpha = \Lambda/\sqrt{2}$ while the thick grey lines correspond to $\alpha = \Lambda/2$. The solid dots are obtained for metal with finite permittivity $\varepsilon' = -50$, for $\alpha = \Lambda/\sqrt{2}$, whereas PEC is simulated in the other cases.

The calculated band structures are presented for two values of α, $\alpha = \Lambda/2$ and $\alpha = \Lambda/\sqrt{2}$, and for two values of the depth h, $h = 0.2 \times \Lambda$ (figure 2 a) and $h = 0.4 \times \Lambda$ (figure 2 b). The

#72206 - $15.00 USD Received 20 June 2006; revised 25 August 2006; accepted 26 August 2006

air light line, (thin dark line), defines the domain between two regions : the modes above the light line (shaded region) are leaky as they can couple with radiation. Thus, only modes with frequency below the light line are really confined at the surface and are of real interest for us.

The existence of surface modes with a corrugated PEC surface is clearly established by the diagrams, since for each structure there is at least one mode below the light line. Band flattening is remarkable between $h = 0.2 \times \Lambda$ and $h = 0.4 \times \Lambda$.

Fig. 3 represents the Electric Field distribution of the surface Bloch modes at the high symmetry points. We represent the E_z component as it is the dominant polarisation. We also indicate the polarization of the field with arrows. Both figures correspond to a case with PEC, and $h = 0.2 \times \Lambda$ and $\alpha = \Lambda/\sqrt{2}$. The field is confined in the z direction at the interface PEC/air.

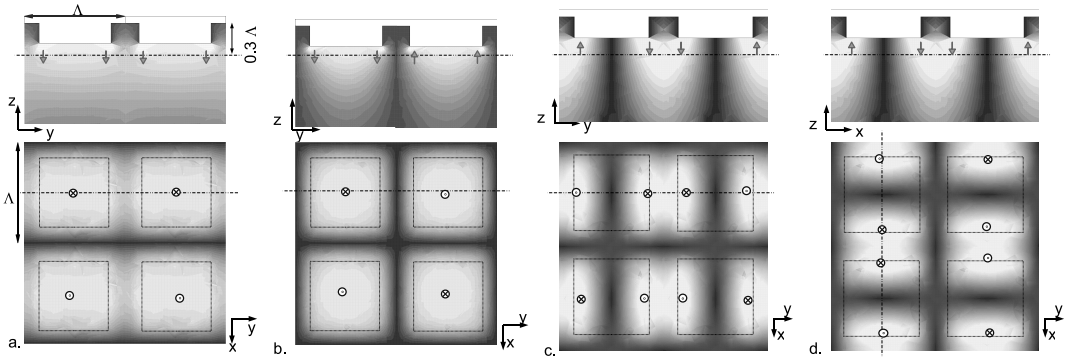

Fig. 3. Magnitude of the E_z field, at an interface PEC/air, on the $x-y$, $z-y$ and $z-x$ planes corresponding to (a) X_X point ($\vec{k} = (\frac{\pi}{\Lambda}, 0)$) and low frequency band, (b) M point, low frequency band, (c) and (d) doubly degenerated M modes of the high frequency band. The depth of the grooves is $h = 0.2.\Lambda$ and $\alpha = \Lambda/\sqrt{2}$. The (x,y) cross-section, represented by a dashed-dotted line on the top figures, is situated at 0.3Λ from the metallic plane. The (y,z) and (x,z) planes are also represented by dashed-dotted lines on the bottom figures, where the dotted square shows the position of the bumps.

Let us first consider the low frequency mode at the X_X and X_Y points, $\vec{k} = (\frac{\pi}{\Lambda}, 0)$ and $\vec{k} = (0, \frac{\pi}{\Lambda})$ respectively, which are doubly degenerated in frequency (see the Brillouin's zone sketched in Fig. 2). The E_z field at the X_X point is periodic with period Λ along the x direction and it is almost invariant along y with anti-nodes centered on the bumps (Fig. 3(a)). Note the changes of sign every Λ in the x direction. The mode at the M point, $\vec{k} = (\frac{\pi}{\Lambda}, \frac{\pi}{\Lambda})$, is represented in figure 3 b, the field changes sign every Λ in both x and y directions and the anti-nodes are centered on the bumps.

A high frequency band appears below the light line near the M point (see. Fig. 2(a)). The upper band mode at the M point is doubly-degenerated in frequency: the field distribution is consistent with the symmetries of the M point, but differs from that of the lower frequency band in the position of the anti-nodes. More specifically, the anti-nodes are centered *between two bumps*, which leaves two possibilities (Fig. 3(c),(d))

We have shown that a PEC surface with an arrays of bumps supports surface waves and exhibit a complete photonic band gap. In this respect, a patterned PEC surface keeps the properties of SPs on corrugated surfaces [2, 15], although the underlying physical mechanism is not related to the plasmon resonance. First of all, we notice that patterning of a PEC surface results in general into a penetration of the electric field with respect to an "average" flat surface. However, there is an important difference between an array of holes, which is considered

#72206 - $15.00 USD Received 20 June 2006; revised 25 August 2006; accepted 26 August 2006

in [6, 7, 8, 9] and an array of bumps. The first case corresponds to simply connected domains into the metal, forming waveguides with a cut-off frequency, which is the key to understand the properties of the surface waves on PEC surfaces. The case of array of bumps is different, as the grooves between the bumps does not form simply connected domains, therefore no cut-off exists.

Several papers on the dispersion properties of sinusoidal, mono-periodical gratings of real metal [12, 13, 2, 14] explain the onset of a photonic bandgap when the effective wavelength of the SP mode is twice the period of the grating, that is $k_x = \pi/\Lambda$ at the X point and $k_x = k_y = \pi/\Lambda$ at the M point. The lower and the upper bands correspond to different field distributions. The field of the low frequency mode is concentrated at the peaks of the grating, while the field of the high frequency mode is concentrated at the troughs; the field lines are more distorted in the latter case and consistently the greater energy stored in the fields by this mode corresponds to a higher frequency [12]. From this point of view, the modes of 2D PEC gratings have the same properties as in 1D gratings, no matter if PEC or not. We notice that, in our 2D case, even the high frequency band exists, with exactly the same kind of field distribution as it would be expected with metal with finite negative permittivity.

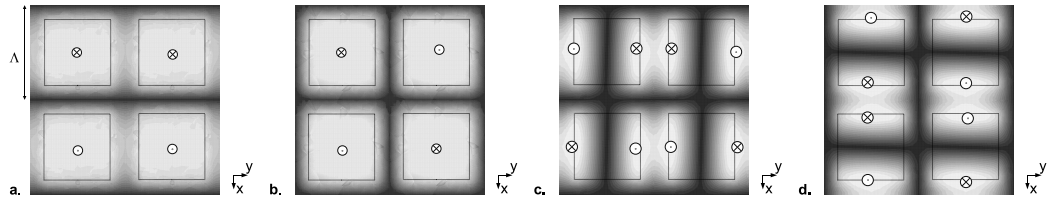

Fig. 4. Magnitude of the E_z field, at an interface metal($\varepsilon = -50$)/air, on the $x-y$ plane corresponding to (a) X_X point and low frequency band, (b) M point, low frequency band, (c) and (d) doubly degenerated M modes of the high frequency band. The depth of the grooves is $h = 0.2.\Lambda$ and $\alpha = \Lambda/\sqrt{2}$. The (x,y) cross-section is situated at 0.3Λ from the metallic plane.

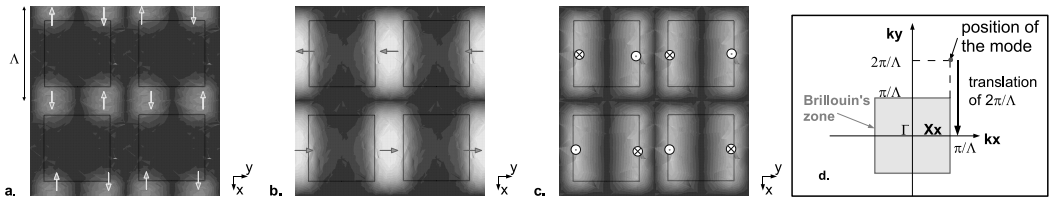

Fig. 5. Field cross sections at the interface metal ($\varepsilon = -50$)/air corresponding to X point and high frequency band : E_x (a), E_y (b) and E_z (c). $h = 0.4\Lambda$ and $\alpha = \Lambda/\sqrt{2}$. The (x,y) cross-section is situated at 0.3Λ from the metallic plane.

To support that, we compare the near infrared with the PEC case ; the real permittivity of the metal is -50 (complex permittivity, thus losses are not taken into account). Only points at the X and M points are calculated, and they are shown with solid dots in Fig. 2. The low and high frequency bands are lower with real metal in the near infrared. The Electric Field distribution of these modes is presented (Fig. 4) for $\alpha = \Lambda/\sqrt{2}$ and $h = 0.2\Lambda$, and is very similar to the case with PEC (Fig. 3).

#72206 - $15.00 USD Received 20 June 2006; revised 25 August 2006; accepted 26 August 2006

It is also interesting to notice that a new mode appears at the X point for a deeper grating ($h = 0.4\Lambda$, Fig. 2(b)). The Electric Field distribution of this mode is shown (Fig. 5) for E_x, E_y and E_z, since, oppositely to the previous cases, E_z is not prevailing on the other fields components ; the antinodes are centered between two bumps. The periodicity $\Lambda/2$ for E_z shows that this mode is of higher order than the mode of Fig. 4(a). We think that it could be the mode situated at $(\pi/\Lambda, 2\pi/\Lambda)$ in the reciprocital lattice, corresponding to the X_X point in the Brillouin zone (Fig. 5(d)). This mode being further from the Γ point, it has a higher frequency than the mode of Fig. 4(a), and thus appears for deeper gratings.

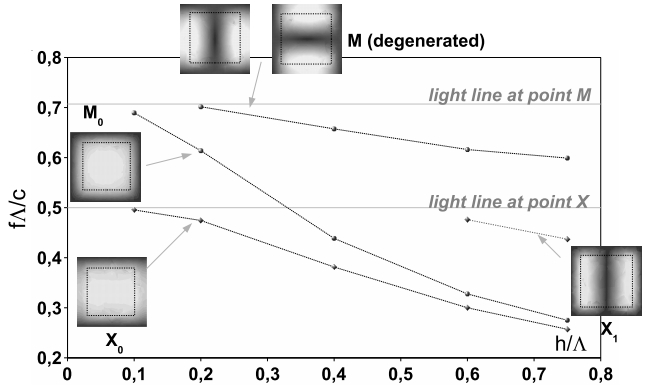

Fig. 6. Position of the modes at the X and M points for several values of $\frac{h}{\Lambda}$ with PEC, for $\alpha = \Lambda/\sqrt{2}$. The corresponding E_z cross-sections in a (x,y) plane are presented near to each set of points. The position of the light line for the X and M points are represented by two grey lines. Index 0 is for the low frequency modes.

Finally, we show in Fig. 6 the positions of the modes at the X and M points for several values of $\frac{h}{\Lambda}$, for a PEC surface and for $\alpha = \Lambda/\sqrt{2}$. The normalized frequency $\frac{f.\Lambda}{c}$ of each set of modes is decreasing when $\frac{h}{\Lambda}$ increases, because the modes become less well bound to the surface, and their energy and thus their frequency is decreased [12]. For nearly shallow gratings ($\frac{h}{\Lambda} = 0.1$), only the low frequency modes exist at the X and M points, and they are very close to the light line. For deeper grooves, the normalized frequency of these modes decreases and a new mode appears at the M point ($\frac{h}{\Lambda} = 0.2$ and 0.4) then at the X point ($\frac{h}{\Lambda} = 0.6$ and 0.75). This X mode has the same field distribution as for real metal (Fig. 5). The existence of this mode labeled X_1 is clearly due to the geometry of the grating, while it only appears for deep grooves. It is interesting to mention here that the causal role for the existence of this mode with real metal (Fig. 5) is played by the geometry of the structure and not by surface plasmons, although SPs may enhance the phenomena.

3. Conclusions

In conclusion, we have investigated the photonic bands of surface modes supported by a PEC structure consisting in an array of bumps. This structure is complementary with the array of holes considered very recently in the litterature. We find that very similar properties, typically associated with surface plasmons, still hold in the long wavelength limit. We conclude that surface gratings, allowing the penetration of the field in the structure, give birth to plasmon-like waves. We think that a better understanding of the properties of surface waves on PEC will be very important for infrared and THz photonics.

#72206 - $15.00 USD Received 20 June 2006; revised 25 August 2006; accepted 26 August 2006